Published in final edited form as:
Carbohydr Polym. 2011 April 22; 85(1): 215–220. doi:10.1016/j.carbpol.2011.02.018.

N,N,N-Trimethyl chitosan nanoparticles for the delivery of monoclonal antibodies against hepatocellular carcinoma cells

Preeyanat Vongchan[1], **Yupanan Wutti-In**[1], **Warayuth Sajomsang**[2], **Pattarapond Gonil**[2], **Suchart Kothan**[3], and **Robert J. Linhardt**[4]

[1]Department of Medical Technology, Faculty of Associated Medical Sciences, Chiang Mai University, Chiang Mai, Thailand [2]National Nanotechnology Center, Nanodelivery System Laboratory, National Science and Technology Development Agency, Pathumthani, 12120 Thailand [3]Department of Radiologic Technology, Faculty of Associated Medical Sciences, Chiang Mai University, Chiang Mai, Thailand [4]Center for Biotechnology and Interdisciplinary Studies and Rensselaer Nanotechnology Center, Rensselaer Polytechnic Institute, New York, USA

Abstract

N,N,N-Trimethyl chitosan chloride is capable of forming nanocomplexes with protein through ionotropic gelation. A monoclonal antibody, raised against human liver heparan sulfate proteoglycan and specifically inhibiting hepatocellular carcinoma *in vitro*, was prepared in nanocomplexes of this modified chitosan. The smallest nanocomplexes (59 ± 17 nm, zeta-potential 16.5 ± 0.5 mV) were obtained at polysaccharide:antibody ratios of 5:0.3. Spherical particles with a smooth surface and compact structure having a mean diameter of ~11.2 ± 0.09 nm were investigated by Atomic Force Microscopy. Cellular uptake of fluorescently labeled nanocomplexes was studied in mouse monocyte models of cancer and normal cells. External and internal fluorescence was analyzed by flow cytometry. The results demonstrate that the nanocomplexes could enter cells and were retained for a longer period of time in cancer cells where they exhibited greater toxicity. These nanocomplexes appear safe and could potentially enhance the half-life of added antibodies.

Keywords

Chitosan; *N,N,N*-Trimethyl chitosan nanocomplexes; Hepatocellular carcinoma; monoclonal antibody; heparan sulfate proteoglycans

1. Introduction

Chitosan is a linear polysaccharide of (1→4) linked 2-amino-2-deoxy-β-D-glucopyranose with an *N*-acetylation degree of typically less than 0.35 (Jollès & Muzzarelli, 1999; Muzzarelli & Muzzarelli, 2005). Chitosan has been widely used as a precursor of non-toxic, biocompatible and biodegradable polysaccharides for use in biomedical applications

Correspondence: Robert J. Linhardt, Phone 518-276-3404; Fax 518-276-3405; linhar@rpi.edu and Preeyanat Vongchan, Phone + 6653 945080 Ext 17; Fax + 6653 946042; preyanat@chiangmai.ac.th.

(Berger, Reist, Chenite, Felt-Baeyens, Mayer & Gurny, 2005). Chitosan, *N*-deacetylated chitin, can be derivatized by *N*-methylation to form *N*, *N*, *N*-trimethyl chitosan (TM-chitosan) chloride (Dillman, Beauregard, Halpern & Clutter, 1986). TM-chitosan chloride, which is a water-soluble compound, can form nanocomplexes with anionic compounds such as drug, proteins, and DNA, through ionotropic gelation, which have potential applications in targeted drug delivery applications (Amidi, Mastrobattista, Jiskoot & Hennink, 2010).

A major limitation of current modalities of cancer treatment is the lack of specificity for cancer cells (Oldham, 1983). Therefore, a major goal in the treatment of cancer is to develop a class of agents with greater specificity for tumor cells. Monoclonal antibodies (MAbs) specific to tumor antigens or tumor-associate antigens offers one such method of highly specific targeting. MAbs can decrease the number of circulating tumor cells, decrease circulating dead cells, and form complexes with circulating tumor antigens (Nadler et al., 1980). MAbs offer a new treatment modality despite problems and limitations, such as clinical toxicity of mouse MAbs (Dillman, Beauregard, Halpern & Clutter, 1986). Their high immunogenicity can induce the production of human anti-mouse antibody or HAMA (Dillman, 1989). Therefore, studies have been directed at preparing mouse humanized antibodies or human antibodies for chemotherapeutic applications (Oldham, 1983; Winter et al., 1993). An alternative approach involves the use of a delivery system to mask or ameliorate the immunogenic effects of therapeutic mouse antibodies.

Hepatocellular carcinoma (HCC) is one of the most common and the third leading cause of cancer deaths in the world (Befeler & Di Bisceglie, 2002; Bruix & Llovet, 2002; Llovet, Burroughs & Bruix, 2003; Okuda, 2000). Late detection and metastasis are major causes of the increasing in death rate in liver cancer. For treatment, surgical resection is currently the most important approach for HCC. However, advanced tumors are often not resectable and metastatic or recurrent tumors also decrease the effectiveness of resection. A number of studies have emphasized the importance of immunotherapeutic strategies against tumors that have been developed over the past 20 years. Mouse MAbs against HCC has been widely applied for tumor imaging, targeting and treatment (Bao et al., 2005; Yu et al., 2005; Zou, Ju & Xie, 2007). These antibodies are also useful tools for the analysis of antigens that might have clinical applications in diagnosis as well as immunotherapy. However, using of antibodies from murine source has a disadvantage in inducing HAMA following their repeated administration. The short biological half-life and associated adverse effects of murine MAbs make these the ideal candidate for controlled drug-delivery systems (Domb, Bentolila & Teomin, 1998; Dunn, Ward, McNeal, Cross & Greenberg, 1993; Hayashi, Haneji, Hamano & Yanagi, 1994). In addition, there have been reports that polymeric materials are suitable for the controlled delivery of proteins (Domb, Bentolila & Teomin, 1998).

Heparan sulfate proteoglycans (HSPGs) have been implicated as playing major roles in tumor biology. HSPGs mediate adhesion and migration as well as cellular responses to mitogenic and angiogeneic growth factors (Blackhall, Merry, Davies & Jayson, 2001). Moreover, HSPGs are critical regulators of tumor invasion and metastasis (Sanderson, 2001) through their HS glycosaminoglycan side chains that encode recognition sites for numerous heparin-binding proteins, such as fibroblast growth factors (Ostrovsky et al., 2002), vascular endothelial growth factor (Robinson & Stringer, 2001) and hepatocyte growth factor/scatter factor (Lyon, Deakin, Rahmoune, Fernig, Nakamura & Gallagher, 1998; Lyon & Gallagher, 1994). HSPG from human liver has been isolated and characterized to solve some questions concerning the molecular interaction of HS in the normal hepatic cells with its protein-based receptors and ligands and with pathogen proteins (Vongchan, Warda, Toyoda, Toida, Marks & Linhardt, 2005). MAb 1E4-1C2 raised against HSPG isolated from human liver reacts with various solid tumor cell lines including HepG2. In a previous attempt by our group to

characterize its biological properties, we found that the 1E4-1C2 could inhibit proliferation of HepG2 cells *in vitro* and reduce tumor mass in athymic nude mice implanted with HepG2 cells. However, a major problem of the 1E4-1C2 MAb is short half-life in blood circulation as well as production of HAMA. In order to solve this problem, the TM-chitosan was synthesized as a carrier to deliver and encapsulate the 1E4-1C2 MAb in a form of antibody-based nanocomplexes to tumor cells.

2. Experimental

2.1. Materials and reagents

Chitosan (Ch) with an average molecular weight (M_w) of 276 kDa was purchased from Seafresh Chitosan (lab) Co., Ltd. in Thailand. The degree of deacetylation (DDA) of chitosan was determined to be 94% by ^{1}H-NMR spectroscopy (Lavertu et al., 2003). A dialysis tubing with M_w cut-off of 12,000–14,000 from Cellu Sep T4 (Membrane Filtration Products, Inc, Segiun, TX, USA) was used to purify TM-chitosan. Iodomethane, *N*-hydroxysuccinimide (NHS) and 1-methyl-2-pyrrolidone were purchased from Acros Organics (Geel, Belgium). Sodium iodide was purchased from Carlo Erba Reagent (Italy. Dimethylsulfoxide (DMSO) and 1-ethyl-3-(3-dimethylaminopropyl)carbodiimide (EDC) were purchased from Sigma-Aldrich (USA). All chemicals and solvents were used as received without any further purification.

HepG2 cell line (human hepatocellular carcinoma) was purchased from CLS Cell Lines Service (Germany). J774 cell line (Mouse macrophages) was a kind gift from Dr. Kanittha Taneyhill, Division of Clinical Chemistry, Department of Medical Technology, Faculty of Associated Medical Sciences, Chiang Mai University.

2.2. Instrumentation

All attenuated total reflectance Fourier transform infrared (ATR-FTIR) spectra were collected with a Nicolet 6700 spectrometer (Thermo Company, USA) using the single-bounce ATR-FTIR spectroscopy (Smart Orbit accessory) with a diamond internal reflection element (IRE) at the ambient temperature (25°C). These spectra were collected by using rapid-scan software in OMNIC 7.0 with 32 scans and a resolution of 4 cm^{-1}. The ^{1}H-NMR spectra were measured on AVANCE AV 500 MHz spectrometer (Bruker, Switzerland). All measurements were performed at 300 K, using the pulse accumulation of 64 scans and LB parameter of 0.30 Hz. D_2O/CD_3COOD and D_2O were used as the solvents for dissolving 5 mg of Ch and TM-chitosan, respectively.

2.3. Synthesis of the N,N,N-trimethyl chitosan chloride (TM-chitosan)

Methylation of Ch was carried out by a single treatment with iodomethane in the presence of *N*-methyl pyrrolidone (NMP) and sodium hydroxide (Sajomsang, Tantayanon, Tangpasuthadol & Daly, 2008). Briefly, a mixture of chitosan (1 g) and NMP (50 mL) were stirred at the room temperature for 12 h. Then 15% (w/v) of sodium hydroxide (8 mL) and sodium iodide (3 g) were added and stirred at 60°C for 15 min. Subsequently, iodomethane (8 mL) was added in thee portions at 3-h intervals and stirred at 60°C for 24 h. The reaction mixture appeared yellow and clear. The obtained compound was precipitated in acetone (600 mL). The precipitate was then dissolved in 15% (w/v) of sodium chloride to replace the iodide ions with chloride ions. Suspension was subsequently dialyzed with deionized water for 3 days to remove inorganic materials and then freeze-dried to give cotton-liked powder TM-chitosan chloride.

TM-chitosan chloride. ATR-FTIR; ν 3304 (O–H and N–H, GlcN), 2922, 2885, and 2834 (C–H, GlcN), 1470 (C–H, $N^+(CH_3)_3$), 1144 (C–O–C, GlcN), 1047, and 1029 cm^{-1}(C–O,

GlcN). ^{1}H-NMR (D_2O): δ (ppm) 5.4 (br. s; 1H H1′), 4.4-3.0 (br. m; 22H H2–H6, s; 6H *3*, *6-O*–C$\underline{H}_3$; s, 9H $N^+(C\underline{H}_3)_3$), 2.7 (br. m; 6H $N(C\underline{H}_3)_2$), 2.3 (s; 3H $NHC\underline{H}_3$), 1.9 (s; 3H NHAc). ^{13}C-NMR (D_2O): δ (ppm) 96.5 (C1), 77.6 (C4), 74.7 (C5), 68.8 (C5), 60.0-55. (C2 and C6), 54.4 ($N^+(\underline{C}H_3)_3$), 42.7 ($N(\underline{C}H_3)_2$).

2.4. Preparation of the TM-chitosan/1E4-1C2 MAb nanocomplexes

The TM-chitosan/1E4-1C2 MAb nanocomplexes were prepared by using ionotropic gelation method. Briefly, monoclonal antibody (MAb) solution (anti-human liver HSPG, clone 1E4-1C2, 1 mg/mL) and various concentrations of TM-chitosan chloride solution ranging from 6 to 30 mg/mL were prepared in PBS buffer pH 7.4. One mL of MAb solution was gradually added into 2 mL of TM-chitosan chloride solution and stirred for 15 min at room temperature. Reaction was stopped and the solution was then filtered through VertiClean nylon syringe filters 0.45 μm (Vertical chromatography Co., Ltd. Thailand).

2.5. Measurement of particle sizes and zeta-potentials of nanocomplexes

Measurement of particle size, polydispersity index (PDI) and zeta-potential of the TM-chitosan/1E4-1C2 MAb nanocomplexes was determined by using photon correlation spectroscopy (PCS; NanoZS4700 nanoseries, Malvern Instruments, UK). Refractive index of the TM-chitosan/MAb nanocomplexes and water were set at 1.33 and 1.33, respectively. Particle sizes and zeta-potentials were reported as the average of thee measurements at 25°C.

2.6. Molecular weight determination

The weight average molecular weight (M_w), number average molecular weight (M_n), and M_w/M_n of chitosan and its derivatives were determined by gel permeation chromatography (GPC). The GPC consists of Waters 600E Series generic pump, injector, ultrahydrogel linear columns (M_w resolving range 1 to 20,000 kDa), guard column, pullulan as standard (M_w 5.9 to 788 kDa), and refractive index detector (RI). All samples were dissolved in acetate buffer pH 4 and then filtered through VertiPure nylon syringe filters 0.45 μm (Vertical chromatography Co., Ltd. Thailand). AcOH (0.5 M) and 0.5 M AcONa (acetate buffer pH 4) were used as mobile phases at a flow rate of 0.6 mL/min at 30°C. Injection volume of 20 μL was collected.

2.7. Study of particle morphology

The morphology of the TM-chitosan/1E4-1C2 MAb nanocomplexes was analyzed by atomic force microscopy (AFM) (SPA400, Seiko, Japan). TM-chitosan/1E4-1C2 MAb nanocomplexes were prepared as mentioned at the concentration ratio of 5:0.3 (TM-chitosan/1E4-1C2 MAb). Appropriate amount of nanocomplexes was diluted with distilled water at optimal dilution ratio and dropped onto freshly cleaved mica. Sample was placed in an atmosphere until completely dried. Imaging was performed by scanning of 10 μm × 10 μm area in tapping mode using an NSG01 cantilever with 115–190 kHz resonance frequencies and a constant force ranged from 2.5–10 Nm^{-1}. All images were recorded in air at 25°C with scan speed of 1 Hz. The phase image and topology image were used to determine the morphology and particle size of the TM-chitosan/1E4-1C2 MAb nanocomplexes.

2.8. In vitro study of cellular uptake of TM-chitosan/1E4-1C2 MAb nanocomplexes

2.8.1. Preparation of the FITC conjugated TM-chitosan/1E4-1C2 MAb nanocomplexes—Fifty mg of TM-chitosan (0.3 mmol) was dissolved in deionized water (5 mL). Twelve mg of fluorescein isothiocyanate (FITC 0.1 meq/GlcN) was dissolved in dimethylsulfoxide (DMSO, 3 mL) and adjusted to pH of 3.0 with 1M HCl. Six mg of 1-

ethyl-3-(3-dimethylaminopropyl)carbodiimide (EDC, 0.1 meq/GlcN) was then added and stirred at room temperature for 1 h. Then 3.5 mg of *N*-hydroxysuccinimide (NHS, 0.1 meq/GlcN) was added. The reaction mixture was stirred at room temperature for another 15 min. Subsequently, the TM-chitosan chloride solution was added into the reaction mixture and stirred at room temperature for 6 h. Finally, the mixture was dialyzed against distilled water for 2 weeks and lyophilized. FITC conjugated TM-chitosan/1E4-1C2 MAb nanocomplexes were prepared by ionotropic gelation method. Briefly, one mL of MAb solution (clone 1E4-1C2, 1 mg/mL) was gradually added into 2 mL of FITC conjugated TM-chitosan chloride solution (15 mg/mL). The reaction mixture was stirred for 15 min at room temperature. The solution was then filtered through VertiClean nylon syringe filters 0.45 μm (Vertical chromatography Co., Ltd. Thailand) and lyophilized.

2.8.2. Uptake of TM-chitosan/1E4-1C2 MAb nanocomplexes by HepG2 and J774 cells—HepG2 cells were cultured in DMEM (Gibco, USA) supplemented with 10% fetal calf serum until 80% confluent. Culture medium was removed and cells were washed with sterile Ca^{2+}/Mg^{2+} free phosphate buffered saline, pH 7.2 (PBS). Cells were then removed with 0.25% trypsin/0.02%EDTA/ Ca^{2+}/Mg^{2+} free PBS, washed and adjusted to 1×10^5 cell/mL with 10% FCS-DMEM. To address the uptake of TM-chitosan/1E4-1C2 MAb nanocomplexes by monocytes, J774 (mouse monocyte cell lines) was used as a study model. Briefly, J774 cells were cultured in DMEM supplemented with 10% fetal calf serum. Cells were collected, washed with sterile PBS pH 7.2 and adjusted to 1×10^5cell/mL with 10% FCS-DMEM. Cells (HepG2 or J774), 5×10^4 cells/500 μL, were loaded into 24-well tissue culture plate and incubated overnight at 37°C, 5% CO_2 and 95% humidity. Culture medium was then removed and various concentrations of FITC conjugated TM-chitosan/1E4-1C2 MAb nanocomplexes diluted in 5 mM glucose/ Ca^{2+}/Mg^{2+} free PBS were added 500 μL/well. Cells were incubated at 37°C, 5%CO_2 and 95% humidity for 6 different incubation times (0, 30 min, 1 h, 3 h, 6 h and 12 h). After completion of each experiment, cells were collected, counted by trypan blue exclusion assay, washed with Ca^{2+}/Mg^{2+} free PBS and then analyzed by flow cytometer. Fluorescent intensity was recorded before adding of 20 mM $CoCl_2$ (20 μL), analyzed and compared between before and after treatment. To address route of uptake in HepG2 cells, 1E4-1C2 MAb (80 μg/mL) was added 500 μL/well to saturate specific binding sites on cell membrane and incubated for another 1 h prior to remove medium and rinsed with Ca^{2+}/Mg^{2+} free PBS. Various concentrations of FITC conjugated TM-chitosan/1E4-1C2 MAb nanocomplexes diluted in 5 mM glucose/ Ca^{2+}/Mg^{2+} free PBS were then added 500 μL/well. The assay was subsequently performed and analyzed as described.

2.8.3. Cytoxicity of TM-chitosan on HepG2 cells and peripheral blood mononuclear cells—Ten mL of heparinized whole blood was collected from 3 normal healthy donors. Peripheral blood mononuclear cells (PBMCs) were isolated by Ficoll-Hypaque gradient centrifugation technique and washed with sterile RPMI-1640 (GibCo, USA). PBMCs and HepG2 cells (8×10^5 cells/250 μL/well) were separately cultured in RPMI-1640 and DMEM supplemented with 10% fetal calf serum, respectively. TM-chitosan chloride diluted in culture medium was added into cell suspension to a final concentration of 0–80 μg/mL. Cells were incubated for a night at 37°C, 5% CO_2 and 95% humidity. Cells were collected, washed and suspended with 500 μL of sterile PBS pH 7.2 before analysis by flow cytometer. Cell count was performed at 20-second analysis.

3. Results and discussion

N,*N*,*N*-Trimethyl chitosan chloride (TM-chitosan choride) was synthesized through a single methylation reaction with iodomethane under basic conditions. The methylation was based on nucleophilic substitution either the primary amino groups or hydroxyl groups of chitosan.

The degree of quaternization (DQ) was determined by ^{1}H-NMR (Polnok, Borchard, Verhoef, Sarisuta & Junginger, 2004) and found to be 30% ± 3. Besides quaternization, the *N*,*N*-dimethylation, *N*-methylation also occurred to a lesser degree at the primary amino groups and *O*-methylation and at the hydroxyl groups of the Ch, respectively. After methylation, the weight average molecular weight of the TM-chitosan chloride found to be decreased compared to the parent Ch. The weight average molecular weight (M_w), number average molecular weight (M_n) and M_w/M_n of Ch and TM-chitosan were determined by gel permeation chromatography (GPC). The M_n, M_w and M_w/M_n of the parent Ch was found to be 48.71 kDa, 276.06 kDa and 5.67, while the TM-chitosan chloride was 40.95 kDa, 204.57 kDa and 4.99, respectively.

In this study, TM-chitosan/1E4-1C2 MAb nanocomplexes were prepared by using ionotropic gelation method. This technique based on electrostatic interaction between the positively charged from quaternary ammonium group of the TM-chitosan and the negatively charged from carboxylate group of the 1E4-1C2 MAb. The solid samples of TM-chitosan/1E4-1C2 MAb nanocomplexes with various concentrations of TM-chitosan and 1E4-1C2 MAb ratios were characterized by using the single-bounce ATR-FTIR spectroscopy with a diamond internal reflection element (IRE) compared to the parent TM-chitosan and 1E4-1C2 MAb, respectively. The TM-chitosan exhibited FTIR band at wave number of 1470 cm^{-1} due to C–H symmetric bending of the methyl substituent of quaternary ammonium groups (Kim, Choi, Chun & Choi, 1997). The 1E4-1C2 MAb exhibited FTIR bands at wave numbers of 1639 cm^{-1} and 1544 cm^{-1} due to C=O stretching and N–H bending of amide group, respectively. The ATR-FTIR spectra of the TM-chitosan/1E4-1C2 MAb nanocomplexes showed reduction of wave number 1470 cm^{-1} when the concentration ratios of TM-chitosan/1E4-1C2 MAb nanocomplexes decreased. The result revealed that quaternary ammonium groups of the TM-chitosan could be formed nanocomplexes with the carboxylate groups present in the 1E4-1C2 MAb.

The particle sizes and zeta-potentials of formed nanocomplexes at pH 7.4 were investigated at various concentration ratios (Figure 1). The particle sizes of these complexes were in the range of 59 ± 17 to 698 ± 55 nm. The particle sizes of the nanocomplexes tended to decrease with an increase in concentration ratios from 2:0.3 to 5:0.3. However, the particle sizes of the nanocomplexes increased when the concentration ratios increased to 10:0.3. The zeta-potentials of all nanocomplexes ranging from11.5 ± 1.0 to 18.3 ± 1.6 mV were obtained. It was found that the zeta-potentials increased with an increasing in concentration of the TM-chitosan. This was due to increasing in the quaternary ammonium group in the complexes. The zeta-potential is known to be one of the major factors affecting bio-distribution and cellular uptake (Nomura, Nakajima, Kawabata, Yamashita, Takakura & Hashida, 1997). A presence of positive surface charge allows an electrostatic interaction to occur between negatively charged cellular membranes and positively charged complexes (Mansouri et al., 2006). In the present study, the smallest complex, obtained at concentration ratios of 5:0.3, was 59±17 nm with a zeta-potential of 16.5±0.5 mV.

The morphology of the nanocomplexes was examined using AFM at concentration ratio of 5:0.3 of TM-chitosan and 1E4-1C2 MAb (Figure 2). Nanocomplexes with uniform particle size were well dispersed in the solution. The images clearly indicate the presence of spherical particles with a smooth surface and compact structure. The geometric mean diameter obtained from AFM is approximately 11.2 ± 0.09 nm. The AFM images demonstrated that majority of the particles were separated from one another, suggesting that these nanocomplexes were probably ionically stabilized against particle agglomeration, due to the positive charges on their surface. AFM provides images of the particles in their dry state, while in dynamic light scattering (DLS) particle size is measured in solution. The size

determined by DLS includes hydrated layers surrounding the nanocomplexes, and is, therefore, larger than that in dry state size determined by AFM.

3.1. Uptake of TM-chitosan/1E4-1C2 MAb nanocomplexes by HepG2 and J774 cells

The total fluorescence intensity of FITC conjugated 1E4-1C2 compared to FITC conjugated TM-chitosan/1E4-1C2 MAb investigated in HepG2 and J774 cells (viability >95%) are shown in Figure 3(a). The maximum increment of total fluorescence intensity of FITC conjugated 1E4-1C2 incubated with HepG2 cell was 3 hours following with progressive decreased. In contrast, total fluorescence intensity FITC conjugated TM-chitosan/1E4-1C2 MAb was increased as a function of time. To measure intracellular fluorescence intensity, cobalt (II) ion (20 mM) was used as an extracellular fluorescence intensity quencher (Biswas, Bhattacharya & Moulik, 2004; Loetchutinat, Kothan, Dechsupa, Meesungnoen, Jay-Gerin & Mankhetkorn, 2005). Uptake of tested molecules was demonstrated as external to internal fluorescence ratio. The external to internal fluorescence intensity ratio of FITC conjugated 1E4-1C2 MAb compared to FITC conjugated TM-chitosan/1E4-1C2 MAb is shown in Figure 3 (b). In the presence of FITC conjugated 1E4-1C2, the ratio of external to internal fluorescence rapidly increased during first 30 minutes, and then decreased until reaching a steady value at 6–12 h. In contrast, cells incubated with FITC conjugated TM-chitosan/1E4-1C2 MAb showed a slightly increases fluorescence ratio during 0–6 h before reaching a plateau at 6–12 h. These results suggest that free 1E4-1C2 MAb more effectively binds to its specific receptor than the nanocomplexes form. 1E4-1C2 MAb in nanocomplexes form might bind and enter HepG2 cells by either antigen-antibody interaction or facilitation. We saturated 1E4-1C2 MAb specific receptors on HepG2 cells with excess unlabeled 1E4-1C2 MAb (80 μg/mL, according to the concentration providing a maximum fluorescence intensity based on indirect immunofluorescent staining). Cultivation of masked HepG2 cells with FITC conjugated 1E4-1C2 or FITC conjugated TM-chitosan/1E4-1C2 MAb for various times were performed. External to internal fluorescence intensity ratio was determined. The results are shown in Figure 3(c). The ratio of FITC conjugated 1E4-1C2 rapidly increases during 0–30 min, and then gradually decreases until it reaches steady state at 3–6 h. This decrease is continuous until 12 h. The FITC conjugated TM-chitosan/1E4-1C2 MAb, however, increases within an hour, but is still at steady state. These results suggest that TM-chitosan/1E4-1C2 MAb not only were taken into the cell but they could also bind to a receptor on the cell surface. Cellular uptake of 1E4-1C2 MAb and TM-chitosan/1E4-1C2 MAb in unsaturated conditions reach steady state at 6 h while under saturated conditions, steady state was reached in 3 h. A study using normal J774 cells as a model showed a similar pattern of 1E4-1C2 MAb uptake both in free and complex form. Taken together, the designed TM-chitosan/1E4-1C2 MAb could enter both HepG2 and normal monocytes. In addition, intracellular retention period of TM-chitosan/1E4-1C2 MAb is longer than that of free MAb. These results are consistent with the previous report that chitosan nanoparticles accumulate in tumor tissues due to enhanced permeation and retention (Brannon-Peppas & Blanchette, 2004).

3.2. Cytoxicity of TM-chitosan on HepG2 cells and peripheral blood mononuclear cells

Data mentioned above indicate that FITC conjugated TM-chitosan/1E4-1C2 MAb could enter to J774 cells, normal mouse monocytes. Therefore, the TM-chitosan/1E4-1C2 MAb can enter and harm to normal peripheral blood cells if it were used as anti-cancer agent. Chitosan nanoparticles reportedly have anti-tumor activity both *in vitro* and *in vivo* (Qi & Xu, 2006; Qi, Xu, Li, Jiang & Han, 2005), we, therefore, studied the cytotoxicity of TM-chitosan both in target HepG2 and normal blood cells. HepG2 cells and normal PBMCs were separately cultured in the presence or absence of in various concentrations of the TM-chitosan. MTT assay was used as indicator of cell viability. The result showed that at concentrations ranged from 5–80 μg /mL, TM-chitosan displayed less toxicity towards

PBMCs (~10%) than towards HepG2 (~22%) based on proliferation inhibition (Figure 4). This observation suggests that TM-chitosan alone has some cytotoxic effect to target HepG2 cells. A recent study in our laboratory has found that 1E4-1C2 MAb inhibits proliferation of HepG2 cells with an IC_{50} of 12.5 μg /mL (unpublished data). TM-chitosan that is encapsulated with 1E4-1C2 MAb, specifically targeting HepG2 cells, may be beneficial in the treatment of hepatocellular carcinoma cells.

4. Conclusion

The objectives of this works were to design the biocompatible 1E4-1C2 MAb-encapsulated chitosan derivative aimed to apply as cancer-specific drug delivery system. We found that quaternary ammonium groups of the TM-chitosan formed nanocomplexes with the carboxylate group of the 1E4-1C2 MAb. The smallest complexes of 59 ± 17 nm and the zeta-potential of 16.5 ± 0.5 mV was obtained at concentration ratios of TM-chitosan: 1E4-1C2 MAb at 5:0.3. These properties facilitated an electrostatic interaction between negatively charged cellular membranes and the positively charged nanocomplexes. The nanocomplexes obtained were shown to enter both normal and HepG2 target cells. However, the nanocomplexes showed longer intracellular retention in HepG2 cells with lower toxicity towards normal cells. Taken together, 1E4-1C2 MAb in form of nanocomplexes may facilitate the development of specific anti-cancer agents in a biodegradable TM-chitosan encapsulated form.

Acknowledgments

This work was financially supported by Thailand Research Fund (TRF 2006–2008) and National Research Council of Thailand (NRCT 2009–2010).

References

Amidi M, Mastrobattista E, Jiskoot W, Hennink WE. Chitosan-based delivery systems for protein therapeutics and antigens. Advanced Drug Delivery Reviews. 2010; 62:59–82. [PubMed: 19925837]

Bao GQ, Li Y, Ma QJ, He XL, Xing JL, Yang XM, Chen ZN. Isolating human antibody against human hepatocellular carcinoma by guided selection. Cancer Biology & Therapy. 2005; 4:1374–1380. [PubMed: 16319526]

Befeler AS, Di Bisceglie AM. Hepatocellular carcinoma: diagnosis and treatment. Gastroenterology. 2002; 122:1609–1619. [PubMed: 12016426]

Berger J, Reist M, Chenite A, Felt-Baeyens O, Mayer JM, Gurny R. Pseudo-thermosetting chitosan hydrogels for biomedical application. International Journal of Pharmaceutics. 2005; 288:17–25. [PubMed: 15607254]

Biswas S, Bhattacharya SC, Moulik SP. Quenching of fluorescence of 1-hydroxypyrene-3,6,8-trisulfonate (HPTS) by Cu2+, Co2+, Ni2+, I−, and cetylpyridinium (CP+) ions in water/AOT/heptane microemulsion. Journal of Colloidal Interface Science. 2004; 271:157–162.

Blackhall FH, Merry CL, Davies EJ, Jayson GC. Heparan sulfate proteoglycans and cancer. British Journal of Cancer. 2001; 85:1094–1098. [PubMed: 11710818]

Brannon-Peppas L, Blanchette JO. Nanoparticle and targeted systems for cancer therapy. Advanced Drug Delivery Reviews. 2004; 56:1649–1659. [PubMed: 15350294]

Bruix J, Llovet JM. Prognostic assessment and evaluation of the benefits of treatment. Journal of Clinical Gastroenterology. 2002; 35:S138–S142. [PubMed: 12394217]

Dillman RO. Monoclonal antibodies for treating cancer. Annals of Internal Medicine. 1989; 111:592–603. [PubMed: 2672932]

Dillman RO, Beauregard JC, Halpern SE, Clutter M. Toxicities and side effects associated with intravenous infusions of murine monoclonal antibodies. Journal of Bioligal Response Modifiers. 1986; 5:73–84.

Domb A, Bentolila A, Teomin D. Biopolymers as drug carriers and bioactive macromolecules. Acta Polymerica. 1998; 49:526–533.

Dunn SJ, Ward RL, McNeal MM, Cross TL, Greenberg HB. Identification of a new neutralization epitope on VP7 of human serotype 2 rotavirus and evidence for electropherotype differences caused by single nucleotide substitutions. Virology. 1993; 197:397–404. [PubMed: 7692670]

Hayashi Y, Haneji N, Hamano H, Yanagi K. Transfer of Sjogren's syndrome-like autoimmune lesions into SCID mice and prevention of lesions by anti-CD4 and anti-T cell receptor antibody treatment. European Journal of Immunology. 1994; 24:2826–2831. [PubMed: 7957574]

Jollès, P.; Muzzarelli, RAA., editors. Chitin and Chitinases. Basel: Birkhauser Verlag; 1999.

Kim C, Choi J, Chun H, Choi K. Synthesis of chitosan derivatives with quaternary ammonium salt and their antibacterial activity. Polymer Bulletin. 1997; 38:387–393.

Lavertu M, Xia Z, Serreqi AN, Berrada M, Rodrigues A, Wang D, Buschmann MD, Gupta A. A validated 1H NMR method for the determination of the degree of deacetylation of chitosan. Journal of Pharmaceutical and Biomedical Analysis. 2003; 32:1149–1158. [PubMed: 12907258]

Llovet JM, Burroughs A, Bruix J. Hepatocellular carcinoma. Lancet. 2003; 362:1907–1917. [PubMed: 14667750]

Loetchutinat C, Kothan S, Dechsupa S, Meesungnoen J, Jay-Gerin J-P, Mankhetkorn S. Spectrofluorometric determination of intracellular levels of reactive oxygen species in drug-sensitive and drug-resistant cancer cells using the 2',7'-dichlorofluorescein diacetate assay. Radiation Physics and Chemistry. 2005; 72:323–331.

Lyon M, Deakin JA, Rahmoune H, Fernig DG, Nakamura T, Gallagher JT. Hepatocyte growth factor/scatter factor binds with high affinity to dermatan sulfate. Journal of Biological Chemistry. 1998; 273:271–278. [PubMed: 9417075]

Lyon M, Gallagher JT. Hepatocyte growth factor/scatter factor: a heparan sulphate-binding pleiotropic growth factor. Biochemical Society Transactions. 1994; 22:365–370. [PubMed: 7958326]

Mansouri S, Cuie Y, Winnik F, Shi Q, Lavigne P, Benderdour M, Beaumont E, Fernandes JC. Characterization of folate-chitosan-DNA nanoparticles for gene therapy. Biomaterials. 2006; 27:2060–2065. [PubMed: 16202449]

Muzzarelli, RAA.; Muzzarelli, C. Chitosan chemistry: relevance to the biomedical sciences. In: Heinze, T., editor. Advances in Polymer Science. Vol. vol 186. Berlin: Springer Verlag; 2005. p. 151-209.

Nadler LM, Stashenko P, Hardy R, Kaplan WD, Button LN, Kufe DW, Antman KH, Schlossman SF. Serotherapy of a patient with a monoclonal antibody directed against a human lymphoma-associated antigen. Cancer Research. 1980; 40:3147–3154. [PubMed: 7427932]

Nomura T, Nakajima S, Kawabata K, Yamashita F, Takakura Y, Hashida M. Intratumoral pharmacokinetics and in vivo gene expression of naked plasmid DNA and its cationic liposome complexes after direct gene transfer. Cancer Research. 1997; 57:2681–2686. [PubMed: 9205077]

Okuda K. Hepatocellular carcinoma. Journal of Hepatology. 2000; 32:225–237. [PubMed: 10728807]

Oldham RK. Monoclonal antibodies in cancer therapy. Journal of Clinical Oncology. 1983; 1:582–590. [PubMed: 6366145]

Ostrovsky O, Berman B, Gallagher J, Mulloy B, Fernig DG, Delehedde M, Ron D. Differential effects of heparin saccharides on the formation of specific fibroblast growth factor (FGF) and FGF receptor complexes. Journal of Biological Chemistry. 2002; 277:2444–2453. [PubMed: 11714710]

Polnok A, Borchard G, Verhoef JC, Sarisuta N, Junginger HE. Influence of methylation process on the degree of quaternization of N-trimethyl chitosan chloride. European Journal of Pharmaceutics and Biopharmaceutics. 2004; 57:77–83. [PubMed: 14729082]

Qi L, Xu Z. In vivo antitumor activity of chitosan nanoparticles. Bioorganic & Medicinal Chemistry Letters. 2006; 16:4243–4245. [PubMed: 16759859]

Qi LF, Xu ZR, Li Y, Jiang X, Han XY. In vitro effects of chitosan nanoparticles on proliferation of human gastric carcinoma cell line MGC803 cells. World Journal of Gastroenterology. 2005; 11:5136–5141. [PubMed: 16127742]

Robinson CJ, Stringer SE. The splice variants of vascular endothelial growth factor (VEGF) and their receptors. Journal of Cell Science. 2001; 114:853–865. [PubMed: 11181169]

Sajomsang W, Tantayanon S, Tangpasuthadol V, Daly WH. Synthesis of methylated chitosan containing aromatic moieties: Chemoselectivity and effect on molecular weight. Carbohydrate Polymers. 2008; 72(4):740–750.

Sanderson RD. Heparan sulfate proteoglycans in invasion and metastasis. Seminars in Cell & Developmental Biology. 2001; 12:89–98. [PubMed: 11292374]

Vongchan P, Warda M, Toyoda H, Toida T, Marks RM, Linhardt RJ. Structural characterization of human liver heparan sulfate. Biochimica et Biophysica Acta. 2005; 1721:1–8. [PubMed: 15652173]

Winter SF, Sekido Y, Minna JD, McIntire D, Johnson BE, Gazdar AF, Carbone DP. Antibodies against autologous tumor cell proteins in patients with small-cell lung cancer: association with improved survival. Journal of the National Cancer Institute. 1993; 85:2012–2018. [PubMed: 8246287]

Yu B, Ni M, Li WH, Lei P, Xing W, Xiao DW, Huang Y, Tang ZJ, Zhu HF, Shen GX. Human scFv antibody fragments specific for hepatocellular carcinoma selected from a phage display library. World Journal of Gastroenterology. 2005; 11:3985–3989. [PubMed: 15996020]

Zou K, Ju J, Xie H. Novel tumor-associated antigen of hepatocellular carcinoma defined by monoclonal antibody E4-65. Acta Biochimica et Biophysica Sinica (Shanghai). 2007; 39:359–365.

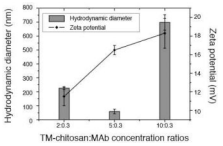

Figure 1.
The particle sizes and zeta-potentials of TM-chitosan:monoclonal antibody (MAb) with various concentrations ratios 2:0.3, 5:0.3 and 10:0.3

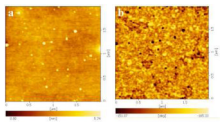

Figure 2.
AFM images of TM-chitosan:monoclonal antibody (MAb) (5:0.3); topology images (a), phase images (b)

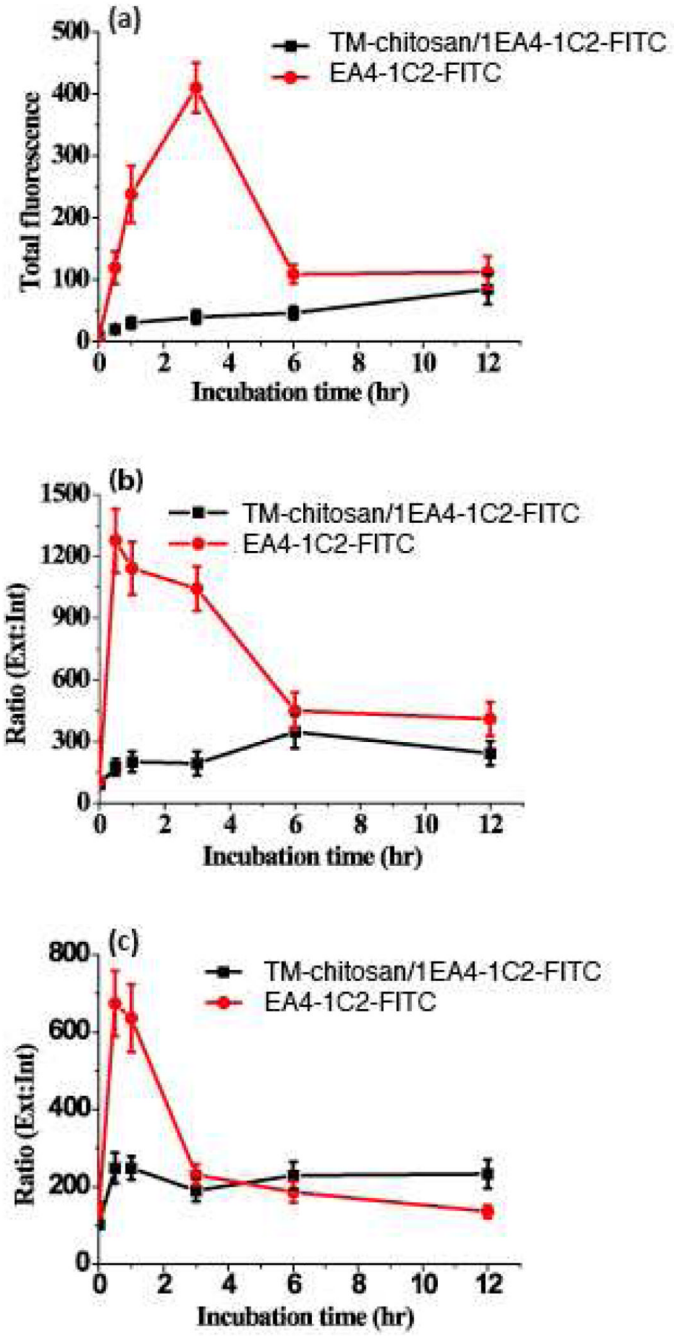

Figure 3.

The fluorescence intensity of TM-chitosan/1E4-1C2-FITC and 1E4-1C2-FITC plots as a function of time. HepG2 cell incubated with TM-chitosan/1E4-1C2-FITC and 1E4-1C2-FITC in various time and then, the total fluorescence intensity were recorded (a). The ratio of external to internal fluorescence intensity of TM-chitosan/1E4-1C2-FITC and 1E4-1C2-FITC were measured (b). In saturation with 1E4-1C2, the total fluorescence intensity of TM-chitosan/1E4-1C2-FITC and 1E4-1C2-FITC in cell were recorded (c).

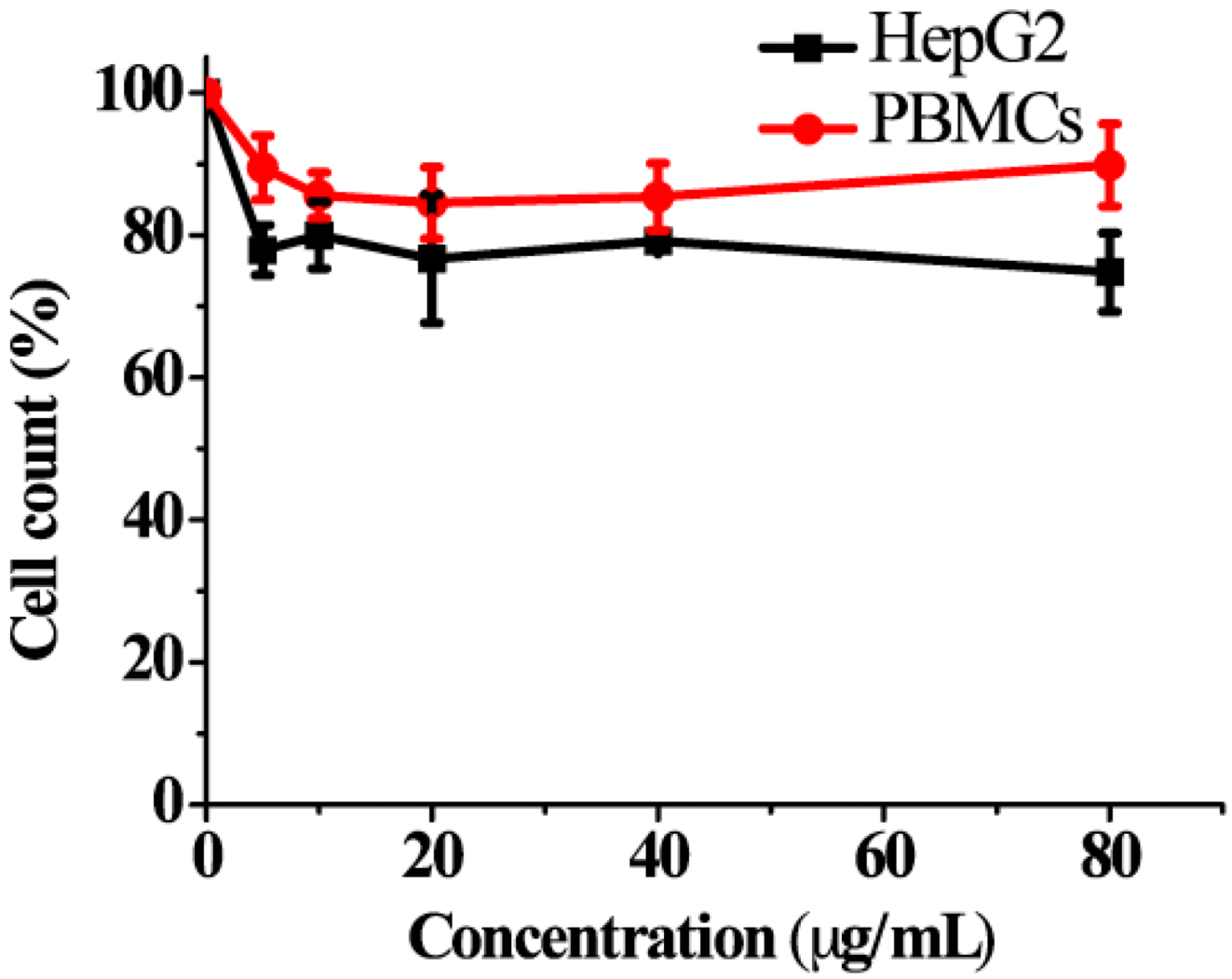

Figure 4.
HepG2 cells and PBMCs were incubated with various concentrations (0–80 μg/mL) of TM-chitosan.